
ETD Archive

2009

Heat Transfer in Electroosmotic Flow of Power-Law Fluids in Micro-Channel

Omkareshwar Rao Bakaraju
Cleveland State University

Follow this and additional works at: <https://engagedscholarship.csuohio.edu/etdarchive>

 Part of the [Mechanical Engineering Commons](#)

How does access to this work benefit you? Let us know!

Recommended Citation

Bakaraju, Omkareshwar Rao, "Heat Transfer in Electroosmotic Flow of Power-Law Fluids in Micro-Channel" (2009). *ETD Archive*. 452.

<https://engagedscholarship.csuohio.edu/etdarchive/452>

This Thesis is brought to you for free and open access by EngagedScholarship@CSU. It has been accepted for inclusion in ETD Archive by an authorized administrator of EngagedScholarship@CSU. For more information, please contact library.es@csuohio.edu.

**HEAT TRANSFER IN ELECTROOSMOTIC FLOW OF
POWER-LAW FLUIDS IN MICRO-CHANNEL**

OMKARESHWAR RAO BAKARAJU

Bachelor of Engineering in Mechanical Engineering

Jawaharlal Nehru Technological University

Submitted in partial fulfillment of requirements for the degree

MASTER OF SCIENCE IN MECHANICAL ENGINEERING

at the

CLEVELAND STATE UNIVERSITY

December, 2009

ACKNOWLEDGEMENTS

I would like to thank my academic advisor and committee chairperson Dr. Rama Subba Reddy Gorla for his continuous guidance, involvement and accessibility during the period of this work.

I would also like to thank my committee members Dr.Majid Rashidi and Dr.Asuquo B Ebiana for their encouragement and their valuable time to review my thesis. I am very grateful to Dr. William J Atherton Interim chair of Mechanical Engineering Department for his support throughout my studies at Cleveland State University.

I would also like to express my gratitude to my parents and my uncle Mr. Hanumanth Rao Padaraju and his family, without his constant support and guidance this milestone in my life would just have remained a dream.

HEAT TRANSFER IN ELECTROOSMOTIC FLOW OF POWER-LAW FLUIDS IN A MICRO-CHANNEL

OMKARESHWAR RAO BAKARAJU

ABSTRACT

The present study examines heat transfer in electro-osmotic flow of power-law fluids in a micro-channel analytically. The boundary layer equations governing the flow of power-law fluids in a micro-channel have been solved. Heat transfer characteristics such as the temperature distribution and Nusselt number are presented for parametric values of electro-kinetic parameter κH (where κ^{-1} is the Debye length and H is semi-channel height of the micro-channel) and Brinkman number. Uniform surface heat flux boundary condition has been considered. The effects of the Brinkman number on the Nusselt number for specific values of the flow behavior index (n) are analytically determined. This analysis has been carried out for two different cases: Case I - $\kappa H < 1$, $0 < \kappa y < 1$, Case II - $\kappa H > 1$, (a) $0 \leq \kappa y < 1$ and (b) $\kappa y > 1$ and the results are presented graphically.

TABLE OF CONTENTS

	Page
ABSTRACT	IV
LIST OF FIGURES	VI
NOMENCLATURE	VII
CHAPTER	
I. Introduction	1
II. Mathematical Formulation and Analysis	5
III. Results and Discussion	28
IV. Conclusions	31
REFERENCES	33
APPENDIX	
A. Figures	36

LIST OF FIGURES

	Page no.
Figure 1. Schematic illustration of electro-osmotically generated flow.	2
Figure 2. Shows a two dimensional slit micro-channel of height $2H$.	5
Figure 3. Temperature distribution for different power-law fluids in a slit microchannel when $0 < \kappa H < 1$.	36
Figure 4. Effect of Br on dimensionless heat transfer rate in a slit microchannel.	37
Figure 5. Effect of Br on dimensionless heat transfer rate for different power-law fluids.	38
Figure 6. Effect of power-law index n and Br on dimensionless heat transfer rate when $0 < \kappa y < 1$.	39
Figure 7. Effect of Br on temperature distribution for different power-law fluids when $\kappa y > 1$.	40
Figure 8. Effects of power-law index n and Br on dimensionless heat transfer rate when $\kappa y > 1$.	41

NOMENCLATURE

a	dimensionless constant
Br	Brinkman number
c	dimensionless constant
c_p	specific heat at constant pressure J/Kg.K
E_0	external electric field N/C
F_x	driving force due to the interaction of the applied electric field..... N/m
H	half distance between plates m
k	thermal conductivity W m ⁻² K ⁻¹
Kn	Knudsen number
m	flow consistency index
Nu	Nusselt number
n	viscosity index
q_w	wall heat flux W m ⁻²
T	temperature K
u	velocity m s ⁻¹

Greek symbols

α	thermal diffusivity m ² s ⁻¹
γ	specific heat ration
μ	dynamic viscosity Pa s
ρ	density kg m ⁻³
ρ_e	net charge density C/m
ν	kinematic viscosity m ² s ⁻¹
θ	dimensionless temperature

ψ_w	zeta potential	mV
κ^{-1}	Debye length	m
Γ	rate of strain tensor	
τ	Shear stress	(Pa)-N/m ²
η	dimensionless vertical coordinate	
ε	dielectric constant	

Subscripts

m	mean
av	average
w	wall

CHAPTER I

INTRODUCTION

Heat transfer in electro-osmotic generated flow of non-Newtonian fluids finds applications in micro-electronics, biomedical diagnostic techniques and a number of other applications. The emerging lab-on-a-chip micro-fluidic devices are getting more attention in medical, pharmaceutical and defense applications due to their low cost, less operation time, light weight and small size.

Research in heat transfer and flow phenomena in micro-channels has become increasingly challenging. Theoretical predictions in this field agree fairly well with known experimental data related to heat transfer in the conventional size channels. The development of micro-mechanics during the last decades stimulated a great interest in heat transfer studies in micro-channels. A number of theoretical and experimental investigations devoted to this problem are carried out from 1994. These details are reported by Yarín [1]. Data on heat transfer in laminar and turbulent flows in micro-channels of different geometry were obtained. Several special problems related to heat transfer in micro-channel were

discussed, including the effect of axial conduction in the wall and viscous dissipation effect. Beskok and Karniadakis [2] defined four different flow regimes based on the value of the Knudsen number, Kn : continuum flow (ordinary density levels) for $Kn \leq 0.001$; slip-flow regime (slightly rarefied) for $0.001 \leq Kn \leq 0.1$; transition regime (moderately rarefied) for $0.1 < Kn < 10$ and free-molecule flow (highly rarefied) for $10 < Kn < \infty$.

The electro-osmosis is the bulk movement of liquid relative to a stationary surface due to an externally applied electric field and was first observed and reported by Reuss [3] nearly two centuries ago. Most solid substances will acquire a relative electric charge when in contact with an aqueous electrolytic solution, which in turn influences the charge distribution in the solution.

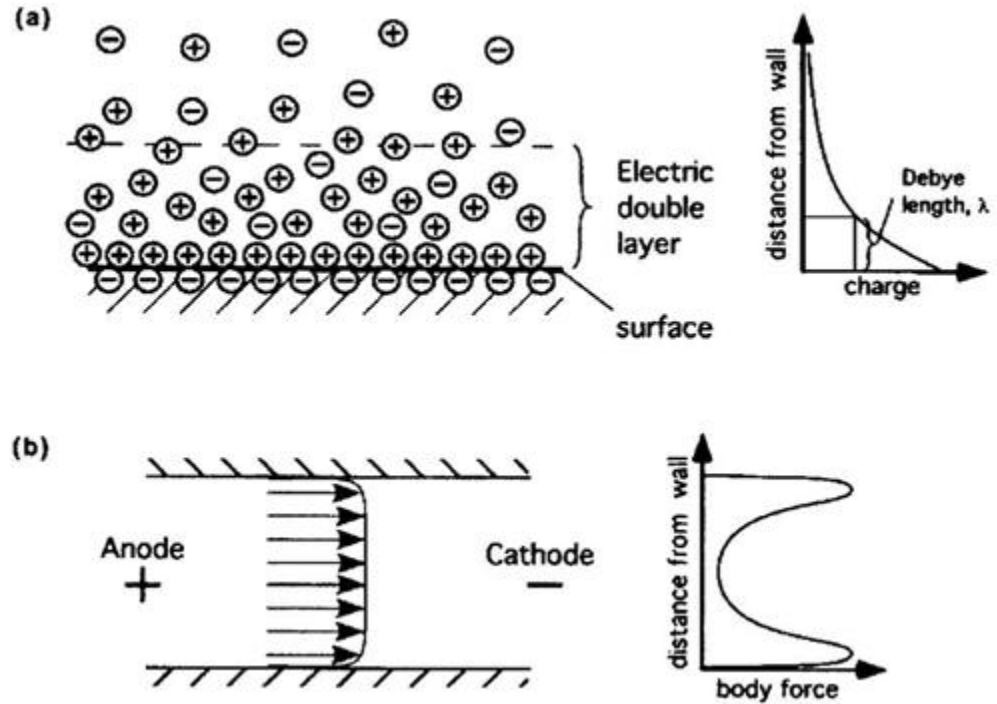


Figure 1. Schematic illustration of electro-osmotically generated flow.

Ions of the opposite charge to that of the surfaces are attracted towards the surface and ions of the same charge are repelled from the surface as shown in Fig 1(a). The net effect is the formation of the region close to the charged surface called the electric double layer (EDL) in which there is an excess of counter ions over anions and which are disturbed in a diffused manner. The charge distribution in fluid therefore falls from its maximum near the wall to the charge in the fluid core. The thickness of ELD is characterized Debye length, which is the wall normal distance over which the net charge has decreased from a magnitude near the tube surface to $1/e$ (37%) of the surface charge. The positively charged cations and solvent molecules strongly absorbed at the wall remain stationary under the influence of an electric potential in the streamwise direction, while the mobile cations in the EDL very near the tube walls will migrate toward the cathode due to the excess charge in the layer. This gives rise to a concentrated fluid body force near the channel or tube walls as illustrated in Fig 1(b). Viscous shear force transmitted from EDL to the channel or tube center pull the core fluid towards the cathode as well. The resulting electro-osmotic flow velocity distribution is a function of the ratio of the hydraulic radius to the Debye length.

Extensive studies of electro-osmotic flow in micro-capillaries have been reported. The power-law model proposed by Kamisli [4], Carreau model proposed by Zimmerman [5], Moldflow first-order model [6] and Bingham model [7] have been successfully developed to analyze non-Newtonian fluid flow and heat transfer. Ghodoossi and Egrican [8] analyzed the heat transfer in a rectangular micro-channel under slip flow approximation. Zimmerman et al. [5] presented a

two-dimensional finite element simulation of electrokinetic flow in a microchannel T-junction for fluid with a Carreau-type nonlinear viscosity. They claimed that the fluid experiences a range of shear rates as it turns around the corner and the flow field was shown to be sensitive to the non-Newtonian characteristics of the Carreau-type. Otevřel and Kleparnik [9] derived the exact solutions for electroosmotic flow in a capillary channel filled with polymer electrolytes having a varying viscosity and the steady state velocity profile was calculated by assuming that the viscosity decreases exponentially in the radial direction. Das and Chakraborty [10] analyzed the electroosmotic flow of a non-Newtonian fluid in microchannel. Chakraborty [11] studied the heat transfer in microtubes under the combined influence of electroosmotic force and pressure gradient.

Zhao et. al. [12] reported an analysis of the electroosmotic flow of power law fluids in a slit microchannel. Aydin and Avic [13] studied the heat transfer in micro-poiseuille flow. The present work has been undertaken in order to study the heat transfer in electroosmotic flow of power-law fluids in a microchannel, for uniform surface heat flux boundary condition the results are analyzed and conclusions are derived.

CHAPTER II

MATHMETICAL FORMULATION AND ANALYSIS

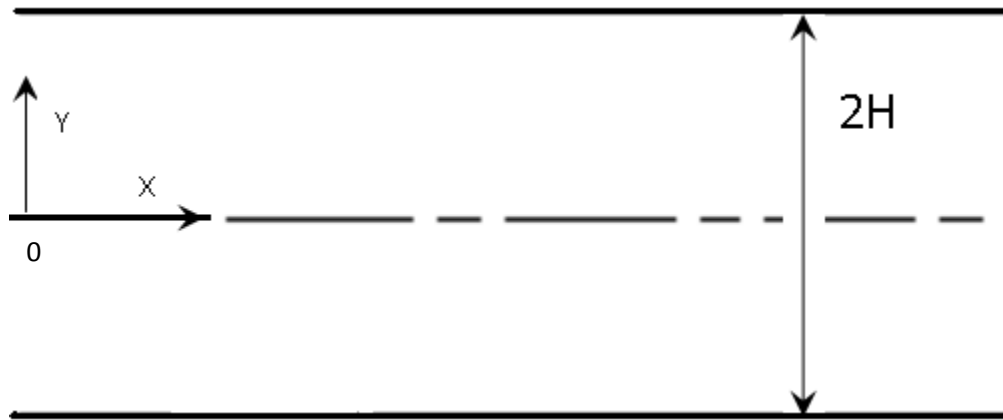


Fig (2) show a two dimensional slit micro-channel of height $2H$.

Derivation of velocity distribution equation's

Consider a microchannel filled with a liquid electrolyte of dielectric constant ϵ . It is assumed that the slit wall is uniformly charged with a zeta potential ψ_w and the liquid solution behaves as a power-law fluid with a flow consistency index m and a flow behavior index n . when an external electric field E_0 is imposed along x direction, the liquid sets in motion due to electro-osmosis.

Because of symmetry, the analysis is restricted to the upper half domain of the slit micro channel.

For electro-osmotic flow, no pressure gradient is applied and gravitational body force is negligible. Thus, the only driving force is due to the interaction of the applied electrical field E_o and the net charge density in the electric double layer (EDL) of the channel wall. Such force acts along x direction and is expressed as:

$$F_x = E_o \cdot \rho_e \quad (1)$$

According to the theory of electrostatics, the net charge density ρ_e in the diffuse layer of the wall EDL is given by the Poisson's equation:

$$\frac{\epsilon d^2 \psi}{dy^2} = -\rho_e \quad (2)$$

With the assumptions of the Boltzmann distribution and small zeta potentials, the electrical potential profile in the EDL is governed by the linearized poisson-Boltzmann equation expressed as:

$$\frac{d^2 \psi}{dy^2} = \kappa^2 \psi \quad (3)$$

The boundary conditions are given by:

$$\psi \big|_{y=H} = \psi_w$$

$$\frac{d\psi}{dy} \bigg|_{y=0} = 0$$

The solution for the electrical potential distribution is given by,

$$\psi(y) = \psi_w \frac{\cosh(\kappa y)}{\cosh(\kappa H)} \quad (4)$$

The net charge density can be expressed as a function of the EDL potential,

$$\rho_e(y) = -\kappa^2 \epsilon \psi \quad (5)$$

The magnitude of strain tensor is defined as:

$$\Gamma = \frac{1}{2} \cdot \frac{d u_x}{d y}$$

The viscosity is defined in terms of velocity gradient as

$$\mu = m (2 \Gamma)^{n-1} = m \left| \frac{d u_x}{d y} \right|^{n-1} = m \left(- \frac{d u_x}{d y} \right)^{n-1} \quad (6)$$

Here, the negative sign is chosen because the velocity decreases with increasing y .

Therefore, the Cauchy momentum equation can be simplified to

$$\frac{d}{d y} \left(m \left(- \frac{d u_x}{d y} \right)^{n-1} \frac{d u_x}{d y} \right) - \kappa^2 \epsilon \psi E_0 = 0 \quad (7)$$

The boundary conditions are given by:

$$u_x \big|_{y=H} = 0$$

$$\frac{du}{dy} \bigg|_{y=0} = 0 \quad (8)$$

Equation (7) is equivalent to

$$\frac{d}{dy} \left(\left(-\frac{du_x}{dy} \right)^n \right) = -\frac{\kappa^2 \varepsilon \psi E_0}{m} \quad (9)$$

Integrating this equation from 0 to y with consideration of the above boundary condition and substituting the electrical potential distribution expressed in equation (4) we have

$$\left(-\frac{du_x}{dy} \right)^n = -\frac{\kappa \varepsilon E_0 \psi_w}{m} \cdot \frac{\sinh(\kappa y)}{\cosh(\kappa H)} \quad (10)$$

The shear stress distribution can be obtained as

$$\tau_{yx} = \kappa \varepsilon E_0 \psi_w \cdot \frac{\sinh(\kappa y)}{\cosh(\kappa H)} \quad (11)$$

From equation (10) the velocity gradient can be expressed as:

$$\frac{d u_x}{d y} = - \left(\frac{-\kappa \varepsilon E o \psi_w}{m} \right)^{\frac{1}{n}} \cdot \left[\frac{\sinh(\kappa y)}{\cosh(\kappa H)} \right]^{\frac{1}{n}} \quad (12)$$

Substituting equation (12) in equation (6) gives the expression for the viscosity of power-law fluids,

$$\begin{aligned} \mu &= m \left(- \frac{d u_x}{d y} \right)^{n-1} \\ &= m^{\frac{1}{n}} (-\kappa \varepsilon E o \psi_w)^{\frac{n-1}{n}} \cdot \left[\frac{\sinh(\kappa y)}{\cosh(\kappa H)} \right]^{\frac{n-1}{n}} \end{aligned}$$

Finally, integrating equation (12) from y to H with the given boundary conditions:

$$u_x \big|_{y=H} = 0$$

$$\frac{du}{dy} \big|_{y=0} = 0$$

Velocity distribution in the channel may be written as:

$$u_x(y) = \kappa^{\frac{(n-1)}{n}} \left(-\frac{\varepsilon E_o \psi_w}{m} \right)^{\frac{1}{n}} \frac{\int_{\kappa y}^{\kappa H} \sinh^{\frac{1}{n}}(\kappa y) d(\kappa y)}{\cosh^{\frac{1}{n}}(\kappa H)} \quad (13)$$

Case I

For $\kappa H < 1$, $0 < \kappa y < 1$;

Integrating equation (13) gives:

$$u_x(y) = n\kappa^{\frac{(n-1)}{n}} \left(-\frac{\varepsilon E_o \psi_w}{m} \right)^{\frac{1}{n}} \cdot \frac{\kappa H^{1+\frac{1}{n}} - \kappa y^{1+\frac{1}{n}}}{\frac{n+1}{\cosh^n(\kappa H)}} \quad (14)$$

The average velocity and the velocity distribution can be obtained respectively as

$$u_{av} = \frac{\int_0^H u \, dy}{H}$$

$$u_{av} = n\kappa^{\frac{(n-1)}{n}} \left(-\frac{\varepsilon E_o \psi_w}{m} \right)^{\frac{1}{n}} \frac{\kappa H^{1+\frac{1}{n}}}{\frac{1+2n}{\cosh^n(\kappa H)}} \quad (15)$$

$$\frac{u}{u_{av}} = \frac{(2n + 1)}{(n + 1)} \left(1 - \left(\frac{y}{H} \right)^{1 + \frac{1}{n}} \right) \quad (16)$$

where, y/H is the dimensionless wall coordinate and n is power-law index.

The conservation of energy including effect of viscosity dissipation is defined as:

$$u \cdot \frac{\partial t}{\partial x} = \alpha \cdot \frac{\partial^2 T}{\partial y^2} + \frac{\nu}{C_p} \left(\frac{\partial u}{\partial y} \right)^{n+1} \quad (17)$$

where, the second term in the right hand side is the viscous dissipation term.

Considering constant surface heat flux boundary condition, we have

$$y = H : \frac{\partial T}{\partial y} = - \frac{q_w}{k} \quad (18)$$

where, q_w is positive when its direction is to the fluid (hot wall) otherwise it is negative (cold wall).

for the uniform wall heat flux condition, we have:

$$\frac{\partial T}{\partial x} = \frac{d T_w}{d x} \quad (19)$$

Defining non-dimensional quantities:

$$\eta = \frac{y}{H}$$

$$\theta = \frac{(T - T_w)}{\left[\frac{q_w \cdot H}{k} \right]}$$

$$\frac{\partial u}{\partial y} = - \frac{(2n + 1)}{n} \cdot \frac{u_{av}}{H} \cdot \eta^{\frac{1}{n}} \quad (20)$$

Substituting equations (16), (18), (19) & (20) in equation (17), we have

$$\begin{aligned}
& \frac{(2n+1)}{(n+1)} \cdot u_{av} \cdot \left[1 - \eta^{\frac{(n+1)}{n}} \right] \cdot \frac{dT_w}{dx} \\
& = \alpha \cdot \frac{d^2\theta}{d\eta^2} \cdot \frac{q_w}{Hk} + \frac{v_l}{Cp} \cdot \left[\frac{(-2n+1)}{n} \cdot \frac{u_{av}}{H} \cdot \eta^{\frac{1}{n}} \right]^{n+1}
\end{aligned}
\tag{21}$$

In dimensionless form, equation (21) may be written as:

$$\frac{d^2\theta}{d\eta^2} = \frac{(2n+1)}{(n+1)} \cdot a \cdot \left[1 - \eta^{\frac{n+1}{n}} \right] + \frac{(2n+1)}{n} \cdot Br \cdot \eta^{\frac{n+1}{n}}
\tag{22}$$

where,

$$a = \frac{u_{av} \cdot Hk}{\alpha \cdot q_w} \cdot \frac{dT_w}{dx} \quad \text{and}$$

$$Br = \frac{v_l}{Cp} \frac{Hk}{\alpha \cdot q_w} \left(\frac{u_{av}}{H} \right)^{n+1}$$

The boundary conditions are given by

$$\eta = 0 \text{ and } \frac{d\theta}{d\eta} = 0;$$

$$\eta = 1 \text{ and } \theta = 0;$$

Integrating equation (22) under the above thermal boundary conditions gives the following expression for the temperature distribution:

$$\theta(\eta) = \frac{1}{2 + 12n^3 + 22n^2 + 12n} \left(-2n^2 Br \left(\eta^{3 + \frac{1}{n}} - 1 \right) (n + 1) \left(\frac{2n + 1}{n} \right)^{n+1} + 12a \left(n + \frac{1}{2} \right) \left(-\frac{1}{3} n^2 \eta^{3 + \frac{1}{n}} + \left(\eta^2 - \frac{2}{3} \right) n^2 + \left(\frac{5}{6} \eta^2 - \frac{5}{6} \right) n + \frac{1}{6} \eta^2 - \frac{1}{6} \right) \right)$$

(23)

Using MATLAB temperature profiles have been shown in Figure (3) with Br and n as parameters.

The mean temperature ($T_m - T_w$) is given by

$$\begin{aligned}
 T_m - T_w &= \frac{\int_0^H \rho \cdot u \cdot (T - T_w) \cdot y}{\int_0^H \rho \cdot u \, dy} \\
 &= \frac{\int_0^1 u \cdot \theta \cdot \frac{q_w \cdot H}{k} \cdot d\eta}{\int_0^1 u \, d\eta} = \frac{q_w \cdot H}{k} \cdot \frac{\int_0^1 u \cdot \theta \cdot d\eta}{\int_0^1 u \, d\eta}
 \end{aligned} \tag{24}$$

Substituting $\theta(\eta)$ and u in equation (10) we have

$$T_m - T_w = \frac{q_w \cdot H}{k} \frac{\frac{3}{10} n Br \left(n + \frac{1}{3} \right) \left(\frac{2n+1}{n} \right)^n - \frac{8}{15} a \left(n^2 + \frac{17}{32} n + \frac{1}{16} \right)}{\left(n + \frac{2}{5} \right) \left(n + \frac{1}{4} \right)} \tag{25}$$

The Nusselt number (Nu) may be written as

$$Nu = - \frac{2}{\theta_m}$$

where mean dimensionless temperature (θ_m) =
$$\frac{(T_m - T_w)}{\frac{q_w \cdot H}{k}}$$

$$\theta_m = \frac{\frac{3}{10} n Br \left(n + \frac{1}{3} \right) \left(\frac{2n+1}{n} \right)^n - \frac{8}{15} a \left(n^2 + \frac{17}{32} n + \frac{1}{16} \right)}{\left(n + \frac{2}{5} \right) \left(n + \frac{1}{4} \right)}$$

(26)

The Nusselt number finally is written as

$$Nu = \frac{12 + 120n^2 + 78n}{-18n Br \left(n + \frac{1}{3} \right) \left(\frac{2n+1}{n} \right)^n + 2a + 32an^2 + 17an}$$

(27)

Case II

For $\kappa H > 1$

Mathematically, the hyperbolic sine function can be approximated as

$$\text{Sinh}(\kappa y) \approx \begin{cases} \kappa y & 0 < \kappa y < 1 \\ \left(\frac{1}{2}\right) e^{\kappa y} & \kappa y > 1 \end{cases} \quad (28)$$

Case II (a): In this case, if $0 \leq \kappa y < 1$. Equation (13) can be integrated piecewise with the above approximation adopted and thus an analytical expression for the velocity distribution can be obtained as:

$$u_x(y) = n\kappa^{\frac{(n-1)}{n}} \left(-\frac{\varepsilon E_o \psi_w}{m} \right)^{\frac{1}{n}} \times \frac{\frac{\left(1 - \kappa y^{1 + \frac{1}{n}}\right)}{n+1} + \frac{\left(e^{\frac{\kappa H}{n}} - e^{\frac{1}{n}}\right)}{2^{\frac{1}{n}}}}{\cosh^{\frac{1}{n}}(\kappa H)} \quad (29)$$

$$u = n \cdot c \cdot \left\{ \frac{\left(1 - \kappa y^{1 + \frac{1}{n}}\right)}{n+1} + R \right\} \quad (30)$$

$$\text{where, } R = \frac{\left(e^{\frac{\kappa H}{n}} - e^{\frac{1}{n}} \right)}{2^{\frac{1}{n}}}$$

$$\text{and } c = \kappa^{\frac{(n-1)}{n}} \left(-\frac{\varepsilon E_o \psi_w}{m} \right)^{\frac{1}{n}} \times \frac{\left(1 - \kappa y^{1 + \frac{1}{n}} \right)}{\frac{n+1}{\cosh^{\frac{1}{n}}(\kappa H)}}$$

Substituting the value of u into the energy equation (17), we have

$$\frac{d^2 \theta}{d \eta^2} = a \cdot n \left\{ \frac{\left(1 - \kappa y^{1 + \frac{1}{n}} \right) \cdot \eta^{1 + \frac{1}{n}}}{n+1} + R \right\} - Br \cdot (\eta \cdot \kappa \cdot H)^{1 + \frac{1}{n}} \quad (31)$$

where,

$$a = \frac{c \cdot k}{\alpha \cdot q_w \cdot H} \frac{d T_w}{d x}$$

$$Br = \frac{v}{C_p} \cdot \frac{k}{\alpha \cdot q_w \cdot H} [c]^{n+1}$$

The boundary conditions are:

$$\eta = 0 \text{ and } \frac{d\theta}{d\eta} = 0;$$

$$\eta = 1 \text{ and } \theta = 0; \quad (32)$$

The energy equation (31) may be integrated by applying the boundary conditions (32) to give the following expression for the temperature distribution:

$$\theta(\eta) =$$

$$\frac{1}{2 + 12n^3 + 22n^2 + 12n} \left(6n \left(-\frac{1}{3} \left(\eta^{3 + \frac{1}{n}} - 1 \right) ((Br + a)n + Br)n(kH)^{1 + \frac{1}{n}} + \left(n + \frac{1}{2} \right) (Rn + 1 + R)(\eta - 1) \left(n + \frac{1}{3} \right) (\eta + 1)a \right) \right)$$

$$(33)$$

Using Matlab the temperature profiles have been shown in figure (7) with Br and n as parameters.

Substituting the values of u and θ in equation (24) we have:

$$\begin{aligned}
 T_m - T_w = & \frac{q_w \cdot H}{k} \times \\
 & - \left(4 \left(H^2 ((Br + a) n + Br) n^2 \left(n + \frac{1}{4} \right) k^2 \left((k H)^{\frac{1}{n}} \right)^2 - 5 \left(\frac{2}{5} \right. \right. \right. \\
 & \left. \left. + n \right) (R n + 1 + R) \left(n + \frac{1}{2} \right) H \left(\left(\frac{1}{2} Br + a \right) n \right. \right. \\
 & \left. \left. + \frac{1}{2} Br \right) n k (k H)^{\frac{1}{n}} + \frac{20}{3} \left(\frac{2}{5} + n \right) (R n + 1 \right. \\
 & \left. \left. + R)^2 a \left(n + \frac{1}{2} \right)^2 \left(n + \frac{1}{4} \right) \right) n \right) / \left((n + 1) (2 n + 1) (2 \right. \\
 & \left. + 5 n) (4 n + 1) \left(2 n + 1 - (k H)^{1 + \frac{1}{n}} n + 2 R n^2 + 3 R n \right. \right. \\
 & \left. \left. + R \right) \right)
 \end{aligned}
 \tag{34}$$

The Nusselt number (Nu) may be written as:

$$Nu = - \frac{2}{\theta_m}$$

where mean dimensionless temperature (θ_m) =
$$\frac{(T_m - T_w)}{\frac{q_w \cdot H}{k}}$$

The Nusselt number finally is written as:

Nu=

$$\frac{1}{2} \left((n+1)(2n+1)(2+5n)(4n+1) \left(2n+1 - (kH)^{1+\frac{1}{n}} n + 2Rn^2 + 3Rn + R \right) \right) / \left(\left(H^2 (Br + a)n + Br \right) n^2 \left(n + \frac{1}{4} \right) k^2 \left((kH)^{\frac{1}{n}} \right)^2 - 5 \left(\frac{2}{5} + n \right) (Rn + 1 + R) \left(n + \frac{1}{2} \right) H \left(\left(\frac{1}{2} Br + a \right) n + \frac{1}{2} Br \right) n k (kH)^{\frac{1}{n}} + \frac{20}{3} \left(\frac{2}{5} + n \right) (Rn + 1 + R)^2 a \left(n + \frac{1}{2} \right)^2 \left(n + \frac{1}{4} \right) \right) n \right) \quad (35)$$

Case II (b): In this case, if $\kappa y > 1$. Equation (13) can be evaluated as

$$u_x(y) = n\kappa^{\frac{(n-1)}{n}} \left(-\frac{\varepsilon E_o \psi_w}{m} \right)^{\frac{1}{n}} \cdot \frac{\frac{\left(e^{\frac{\kappa H}{n}} - e^{\frac{\kappa y}{n}} \right)}{2^{\frac{1}{n}}}}{\cosh^{\frac{1}{n}}(\kappa H)} \quad (36)$$

$$u = \frac{c \cdot n \cdot \left(1 - e^{\frac{\kappa H(\eta-1)}{n}} \right) e^{\frac{\kappa H}{n}}}{2^{\frac{1}{n}}} \quad (37)$$

where,

$$c = \frac{\kappa^{\frac{(n-1)}{n}} \left(-\frac{\varepsilon E_o \psi_w}{m} \right)^{\frac{1}{n}}}{\cosh^{\frac{1}{n}}(\kappa H)}$$

Substituting the value of u into the energy equation (17) we have:

$$\begin{aligned} \frac{d^2\theta}{d\eta^2} = & a \cdot \frac{n}{2^n} \cdot \left(e^{\frac{k \cdot H}{n}} \right) \cdot \left(1 - e^{\frac{k \cdot H}{n}(\eta - 1)} \right) \\ & - (k \cdot H)^{n+1} \cdot Br \cdot \left(\frac{1}{2^n} \right)^{n+1} \cdot \left(e^{k \cdot H \cdot \eta} \right)^{n+1} \end{aligned} \quad (38)$$

where,

$$a = \frac{c \cdot k}{\alpha \cdot q_w \cdot H}$$

$$Br = \frac{v}{C_p} \cdot \frac{k}{\alpha \cdot q_w \cdot H} [c]^{n+1}$$

The boundary conditions are:

$$\eta = 0 \text{ and } \frac{d\theta}{d\eta} = 0;$$

$$\eta = 1 \text{ and } \theta = 0; \quad (39)$$

The energy equation (38) may be integrated by applying the boundary conditions (39) to give the following expression for the temperature distribution:

$$\theta(\eta) =$$

$$\begin{aligned} & \frac{1}{2} \frac{1}{2^n k^2 H^2 (n+1)^2} \left(-2 a n^3 e^{\frac{kH}{n}} (n+1)^2 e^{\frac{kH(\eta-1)}{n}} \right. \\ & \quad + 2 a n^2 k H e^{\frac{kH}{n}} (n+1)^2 (\eta-1) e^{-\frac{kH}{n}} + a (2 n^2 \\ & \quad + k^2 H^2 (\eta-1) (\eta+1)) (n+1)^2 n e^{\frac{kH}{n}} \\ & \quad + 2 \left(\frac{1}{2^n} \right)^{n+1} 2^n \left(- (e^{kH\eta})^{n+1} + (e^{kH})^{n+1} + (\eta \right. \\ & \quad \left. - 1) k H n + (\eta-1) k H \right) (kH)^{n+1} Br \Bigg) \end{aligned}$$

(40)

Using Matlab the temperature profiles have been shown in figure (11) with Br and n as parameters.

The mean temperature is given by:

$$T_m - T_w = \frac{q_w \cdot H}{k} \times$$

$$\begin{aligned} & \frac{1}{6} \left(-3 n (n + 1) \left(a n (n + 1)^2 (-6 n^2 + k^2 H^2) e^{\frac{k H}{n}} \right. \right. \\ & \quad - 2 (2^n)^{-n} k^n H^n k H Br e^{k H (n + 1)} + 2 \left(H k^n H^n k Br (n \right. \\ & \quad + k H) (2^n)^{-n} + \left(\frac{3}{2} n + k H \right) n^2 (n + 1) a \left. \right) (n + 1) \left(1 \right. \\ & \quad + n^2 + n \left. \right) e^{\frac{(n - 1) k H}{n}} - 2 \left(-\frac{3}{2} n^3 - 3 n^2 k H \right. \\ & \quad + k^3 H^3 \left. \right) n (n + 1)^3 a (1 + n^2 + n) e^{\frac{k H (n + 1)}{n}} \\ & \quad - 6 k H n e^{k H} (2^n)^{-n} k^n H^n Br (n + 1) e^{-\frac{k H}{n}} \\ & \quad + 6 n^3 e^{k H} a (1 + n^2 + n) (n + 1)^3 (-3 n + k H) e^{\frac{k H}{n}} \\ & \quad - 6 (2^n)^{-n} k^n H^n Br e^{k H} k H n (n + 1) (1 + n^2 \\ & \quad + n) e^{k H (n + 1)} + 6 H (2^n)^{-n} k^n H^n Br k (2 n^2 k H + n^3 k H \\ & \quad - 1 + 2 k H n + k H) e^{k H (2 + n)} - 3 e^{k H} (1 + n^2 \\ & \quad + n) (Br k H k^n (-2 n^4 - 4 n^3 + (k^2 H^2 - 2) n^2 + 2 k^2 H^2 n \\ & \quad + k^2 H^2 - 2) H^n (2^n)^{-n} + a n^2 (n + 1)^3 (-2 n^2 + k^2 H^2)) \left. \right) \\ & \quad \left(2^n k^2 H^2 (n + 1)^3 (1 + n^2 + n) e^{k H} \left(k H - n \right. \right. \\ & \quad \left. \left. + e^{-\frac{k H}{n}} n \right) \right) \end{aligned}$$

(41)

The Nusselt number (Nu) may be written as:

$$\text{Nu} = -\frac{2}{\theta_m}$$

where mean dimensionless temperature (θ_m) =
$$\frac{(T_m - T_w)}{\frac{q_w \cdot H}{k}}$$

The Nusselt number finally is written as:

$$\begin{aligned} \text{Nu} = & \left(12 \cdot 2^n \cdot k^2 \cdot H^2 \cdot (n+1)^3 \cdot (1+n^2+n) \cdot e^{kH} \left(kH - n \right. \right. \\ & \left. \left. + e^{-\frac{kH}{n}} \cdot n \right) \right) / \left(3 \cdot n \cdot (n+1) \cdot \left(a \cdot n \cdot (n+1)^2 \cdot (-6n^2 \right. \right. \\ & \left. \left. + k^2 H^2) \cdot e^{\frac{kH}{n}} - 2 \cdot (2^n)^{-n} \cdot k^n \cdot H^n \cdot kH \cdot Br \cdot e^{kH(n+1)} \right. \right. \\ & \left. \left. + 2 \left(H \cdot k^n \cdot H^n \cdot kBr \cdot (n+kH) \cdot (2^n)^{-n} + \left(\frac{3}{2} n + kH \right) n^2 \cdot (n \right. \right. \right. \\ & \left. \left. \left. + 1) \cdot a \right) \cdot (n+1) \right) \cdot (1+n^2+n) \cdot e^{\frac{(n-1)kH}{n}} + 2 \left(-\frac{3}{2} n^3 \right. \right. \\ & \left. \left. - 3n^2 kH + k^3 H^3 \right) n \cdot (n+1)^3 \cdot a \cdot (1+n^2+n) \cdot e^{\frac{kH(n+1)}{n}} \right. \\ & \left. \left. + 6kHn \cdot e^{kH} \cdot (2^n)^{-n} \cdot k^n \cdot H^n \cdot Br \cdot (n+1) \cdot e^{-\frac{kH}{n}} \right. \right. \\ & \left. \left. - 6n^3 \cdot e^{kH} \cdot a \cdot (1+n^2+n) \cdot (n+1)^3 \cdot (-3n+kH) \cdot e^{\frac{kH}{n}} \right. \right. \\ & \left. \left. + 6 \cdot (2^n)^{-n} \cdot k^n \cdot H^n \cdot Br \cdot e^{kH} \cdot kHn \cdot (n+1) \cdot (1+n^2 \right. \right. \\ & \left. \left. + n) \cdot e^{kH(n+1)} - 6H \cdot (2^n)^{-n} \cdot k^n \cdot H^n \cdot Br \cdot k \cdot (2n^2 kH + n^3 kH \right. \right. \\ & \left. \left. - 1 + 2kHn + kH) \cdot e^{kH(2+n)} + 3 \cdot e^{kH} \cdot (1+n^2 \right. \right. \\ & \left. \left. + n) \cdot (Br \cdot kH \cdot k^n \cdot (-2n^4 - 4n^3 + (k^2 H^2 - 2) n^2 + 2k^2 H^2 n \right. \right. \\ & \left. \left. + k^2 H^2 - 2) \cdot H^n \cdot (2^n)^{-n} + a n^2 \cdot (n+1)^3 \cdot (-2n^2 + k^2 H^2) \right) \right) \end{aligned} \quad (42)$$

CHAPTER III

RESULTS AND DISCUSSION

The electrokinetic parameter (κH), power-law index (n) and Brinkman number (Br) are the main parameters governing the heat transfer in microchannel. These effects for the case I ($\kappa H < 1$, $0 < \kappa y < 1$) are shown in figures 3 and 4. Figure 3(a) shows the temperature distribution for negative values of Br whereas Figure 3(b) shows the temperature distribution for positive values of Br . The temperature is maximum at the center of the channel and decreases towards the wall. When $Br < 0$ pseudoplastic fluids have higher temperature, whereas dilatant fluids have higher temperature for $Br > 0$. This is because of the viscous dissipation which is grater in dilatant fluids than that in pseudoplastic fluids.

Figures 4(a) and 4(b) show the variation of the Nusselt number with the power-law index for different values of Br . The heat transfer rate decreases as the power-law index increases for high values of Br , whereas it displays opposite behavior for negative values of Br and dilatant fluids. Positive Br correspond to hot wall ($T_w < T_c$), whereas the negative values of Br correspond to cold wall ($T_w > T_c$). Figure 4(a) shows that Nu increases with decreasing values of Br . This is

because viscous dissipation aids heat transfer for the wall cooling case. Figure 4(b) shows that Nu decreases for all values of n due to larger values of the constant “ a ”. The heat transfer rate is influenced more for pseudoplastic fluids by Br .

The effects of the main parameters on the local temperature and heat transfer rates are shown in figure 5 and 6 for case II ($0 < \kappa_y < 1$ and $\kappa_H > 1$). Figure 5(a) and 5(b) show the temperature distribution for different power-law fluids when $Br < 0$ and $Br > 0$, respectively. In both figures, the temperatures for pseudoplastic fluids are higher than dilatant fluids. The temperature is maximum at the center and decreases towards the wall value. Figure 5(b) shows that the temperature is higher as Br increases. The effect of electro-kinetic parameter κ_H and Br on the Nusselt number are shown in Figure 6(a) and 6(b) for pseudoplastic and dilatant fluids respectively. The dimensionless heat transfer rate is independent of κ_H for higher values of κ_H . However for smaller values of κ_H , Nu increases with Br . For $Br < 0$, Nu increases with κ_H , whereas for $Br > 0$, Nu decreases for smaller values of κ_H and increases for larger values of κ_H .

The temperature distribution and heat transfer rates for $\kappa_H > 1$ and $\kappa_y > 1$ are shown in Figures 7 and 8. Figure 7 shows the effect of n and Br on the dimensionless temperature for $\kappa_H = 2$. It is observed that pseudoplastic fluids have lower temperature than dilatant fluids. As in the previous cases, the temperature is maximum at the center and decreases towards the wall. It can also be observed that the temperature increases with Br . Figures 8(a) and 8(b) show

the variation of Nu with the electro-kinetic parameter κH for pseudoplastic and dilatant fluids, respectively. It is clearly seen that the heat transfer rate of pseudoplastic fluids increases with κH for all values of Br , whereas it increases for $Br > 0$ and decreases for $Br < 0$ in the case of dilatant fluids.

CHAPTER IV

CONCLUSIONS

In this study we have presented a mathematical model for describing the heat transfer in electro-osmotic flow of power-law fluids in micro-channel. While considering a uniform surface heat flux boundary condition, we solved the boundary layer equations governing the fluid flow in the micro-channel and presented the results graphically in terms of Nusselt number, Brinkman number and dimensionless temperature. From the analysis of the results obtained, the following important inferences can be drawn:

- The viscous dissipation effect in fluids is observed only when $\kappa H < 1$.
- The heat transfer rate decreases as the power-law index increases for high values of Br whereas it displays opposite behavior for dilatant fluids.
- For higher values of κH no effect of hot wall (Positive Br correspond to hot wall ($T_w < T_c$)) or cold wall (negative values of Br correspond to cold wall ($T_w > T_c$)) on the rate of heat transfer is seen.
- For smaller values of κH , Nu increases with Br (when $Br < 0$) and Nu decreases with Br (when $Br > 0$).

- For $\kappa y > 1$, Br has no significant effect on the temperature distribution in the channel.
- For $\kappa y > 1$, the magnitude of the heat transfer is less compared to the heat transfer for $0 < \kappa y < 1$.

REFERENCES

- [1] L.P.Yarin, Fluid flow, “Heat transfer and boiling in micro-channels”, Springer, 2009.
- [2] A.Beskok,G.E.Karinadakis , “Simulation of heat and momentum transfer in complex micro-geometries”, Journal of Thermophysics Heat Transfer 8(1994) 355-370.
- [3] F.F. Reuss, “Charge-induced flow”, Proc.Imp. Soc. Natural, Moscow 3(1809) 327-344.
- [4] F.Kamisli, “Flow analysis of a power-law fluid confined in an extrusion die”, International Journal of Engineering Science, 41(2003) 1059.
- [5] W.B.Zimmerman, J.M.Rees, T.J.Craven, “Microfluidics and Nanofluidics”, Journal, 2 (2006) 481-492.
- [6] Y.H.Koh, N.S. Ong, X.Y.Chen, Y.C.Lam, J.C.Chai, “Effect of viscous dissipation on the temperature of the polymer during injection molding filling”, Int. Journal Commun. Heat and Mass transfer, 31 (2004) 1005.
- [7] M.Das, V.K.Jain, P.S.Ghoshdastidar, “Fluid flow analysis of magnetorheological abrasive flow finishing (MRAFF) process”, Int. J.Mach. Tool manufacturing, 48 (2008) 415.
- [8] Lotfollah Ghodoossi, Nilüfer Eğrican,” prediction of heat transfer characteristics in rectangular microchannels for slip flow regime and H1

- boundary condition”, *International Journal of Thermal Sciences*, 44 (2005) 513-520.
- [9] M.Otevřel, K. Kleparnik, “Electroosmotic flow in capillary channels filled with nonconstant viscosity electrolytes: Exact solution of the Navier-Stokes equationElectrophoresis”, *Journal of Symposium Miniaturization Innovations* 23(2002) 3574.
- [10] S.Das, S.Chakraborty, “Analytical solutions for velocity, temperature and concentration distribution in electroosmotic microchannel flows of a non-Newtonian bio-fluid”, *Analytica Chimica Acta*, 559 (2006) 15-24.
- [11] Suman Chakraborty, “Analytical solution of Nusselt number for thermally fully developed flow in microtubes under a combined action of electroosmotic forces and imposed pressure gradients” *International Journal of Heat and Mass Transfer*, 49 (2006) 810-813.
- [12] Cunlu Zhao, Emilijk Zholkovskij, Jacob H.Masliyah, Chun Yang, “Analysis of electroosmotic flow of power-law fluids in a slit microchannel”, *Journal of Colloid and Interface Science*, 326 (2008) 503-510.
- [13] Orhan Aydin and Mete Avci, “Analysis of laminar heat transfer in micro-poiseuille flow”, *International Journal of Thermal Sciences*, 46 (2007) 30-37.

APPENDIX

APPENDIX A

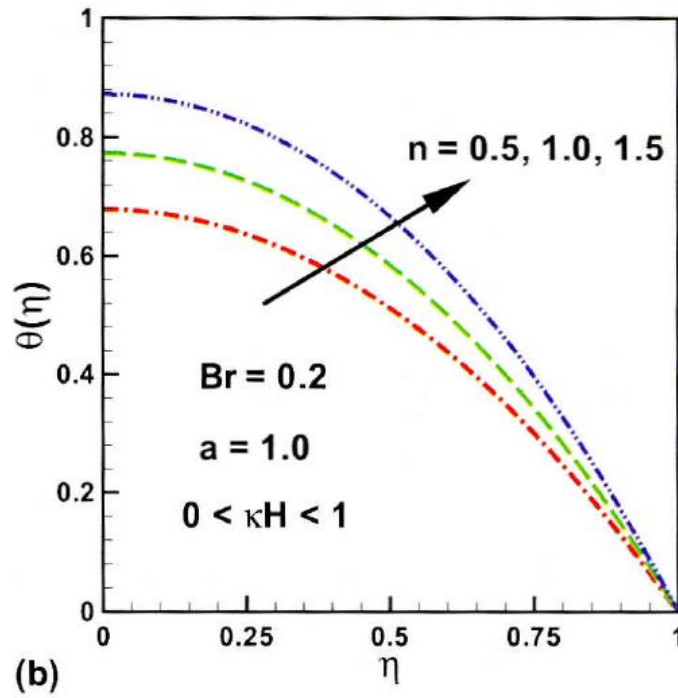
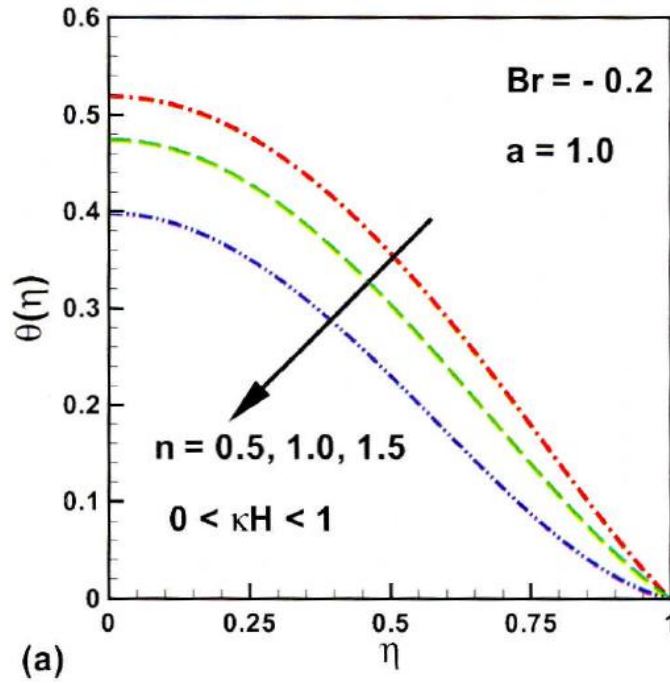


Figure 3. Temperature distribution for different power-law fluids in a slit microchannel when $0 < \kappa H < 1$.

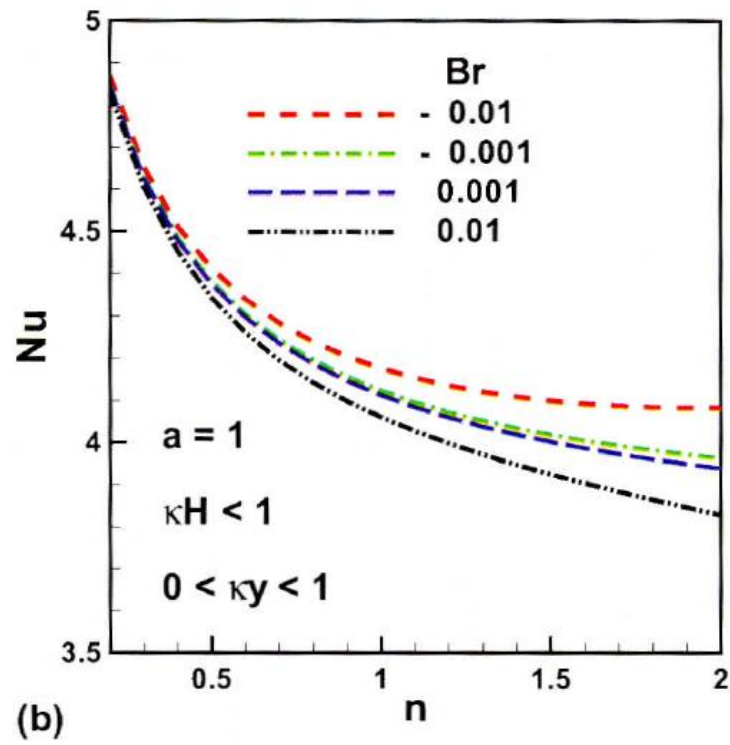
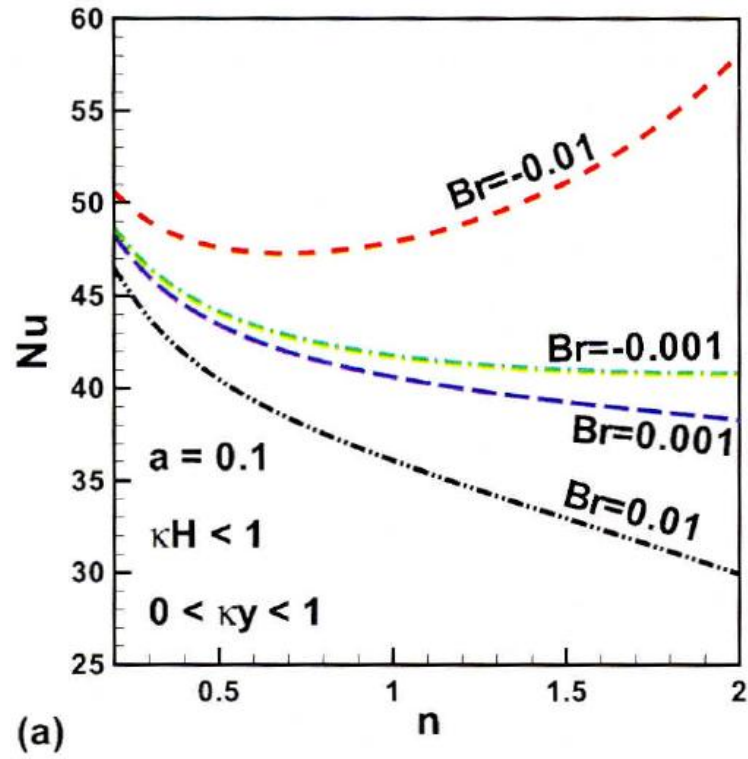


Figure 4. Effects of Br on dimensionless heat transfer rate in a slit microchannel.

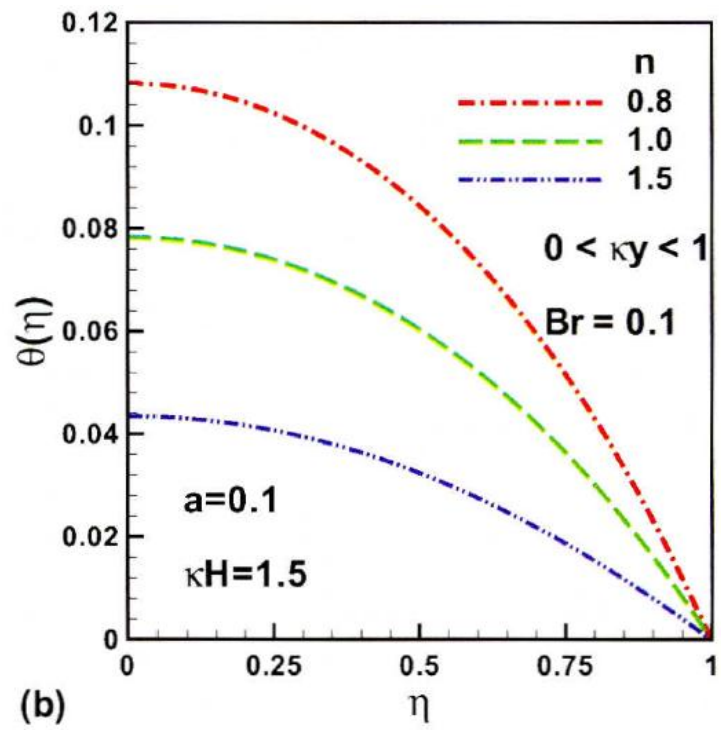
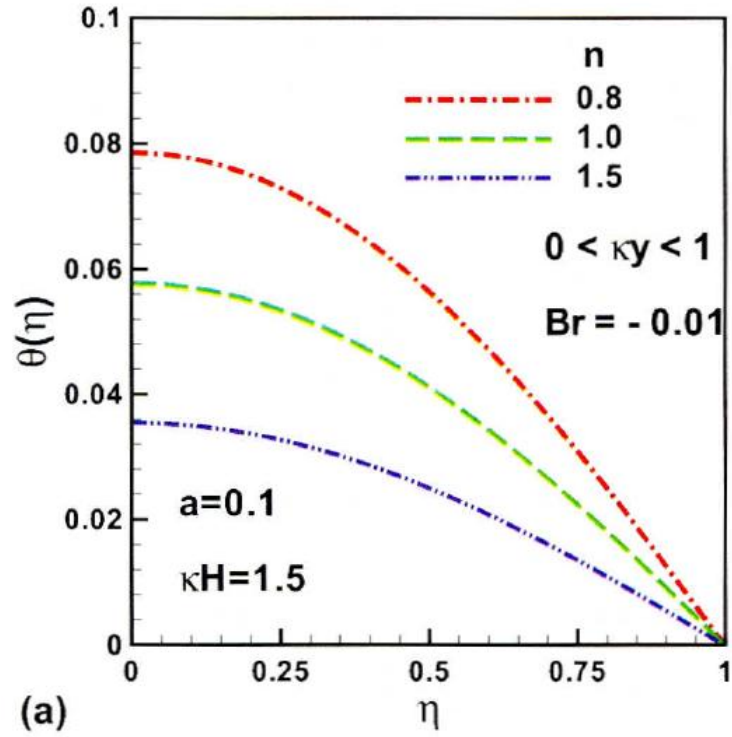


Figure 5. Temperature distribution for different power-law fluids in a microchannel, when $\kappa H > 1$ and $\kappa y < 1$.

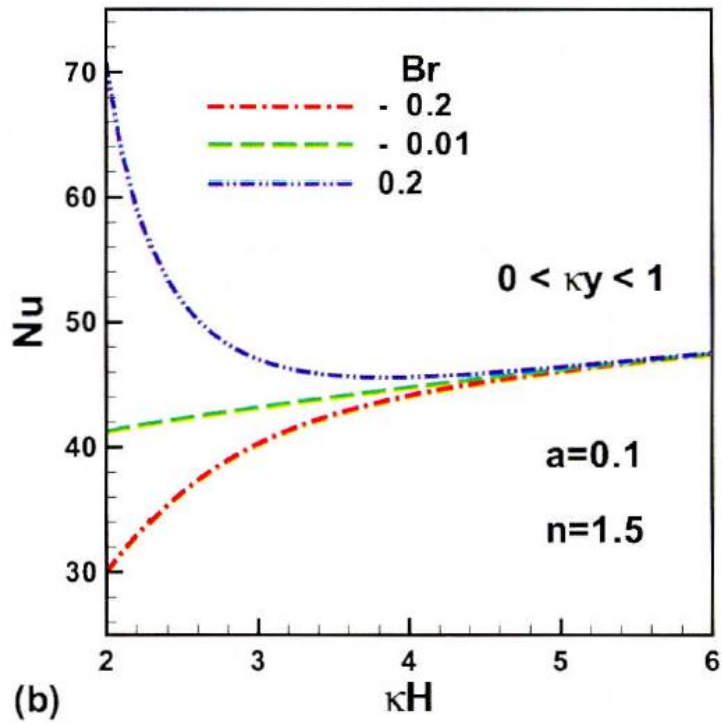
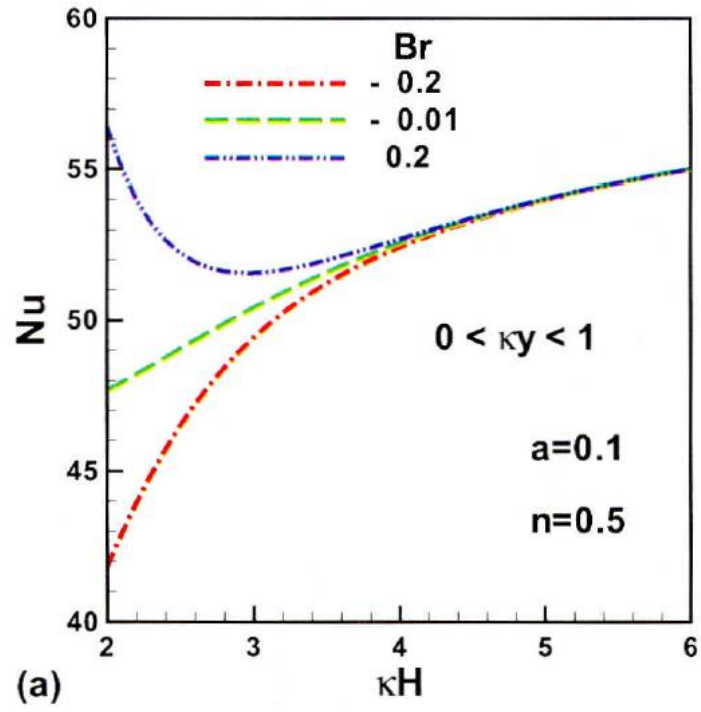


Figure 6. Effects of power-law index n and Br on dimensionless heat transfer rate when $0 < \kappa y < 1$.

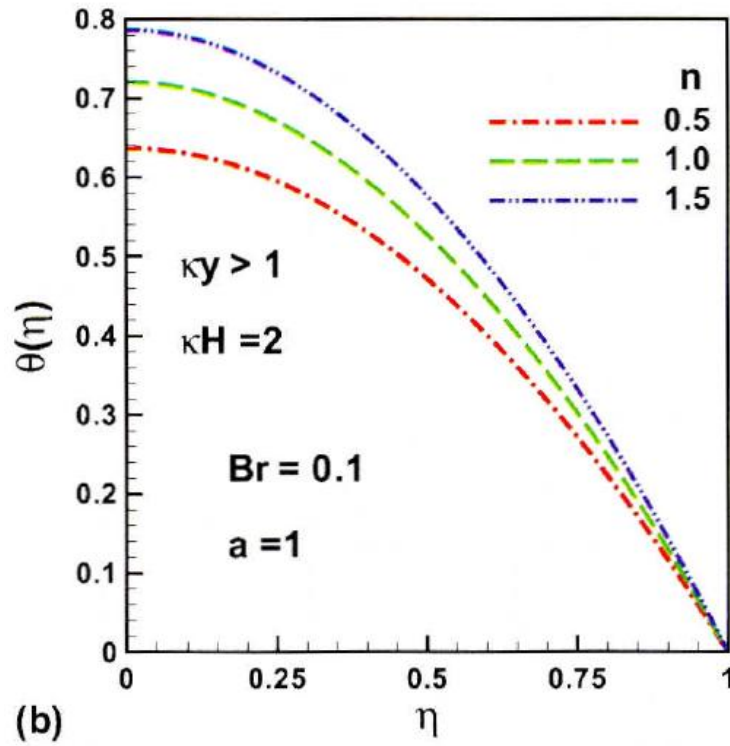
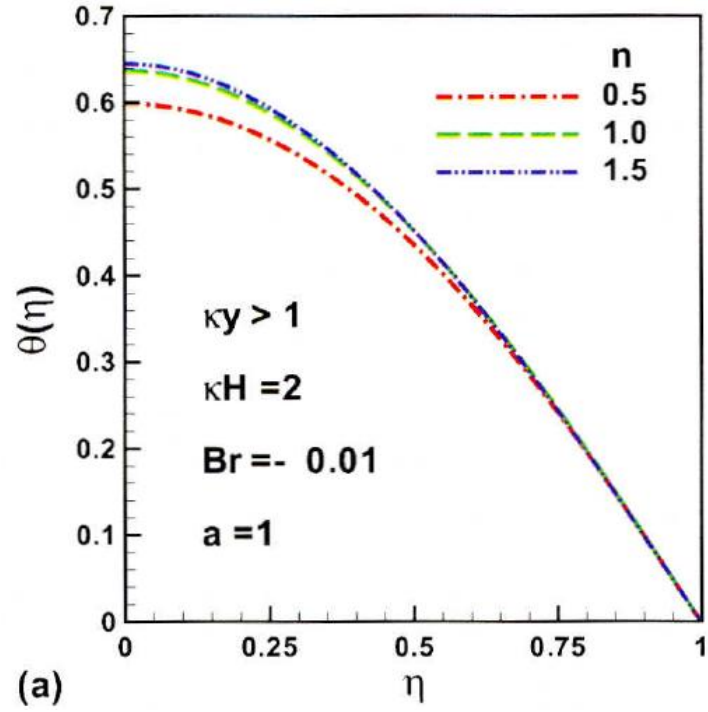


Figure 7. Effects of Br on temperature distribution for different power-law fluids

when $\kappa\gamma > 1$.

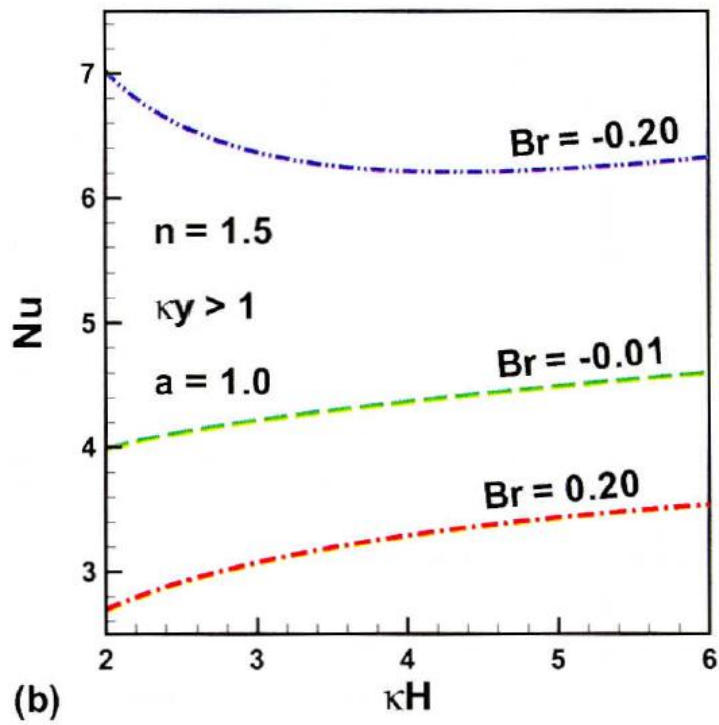
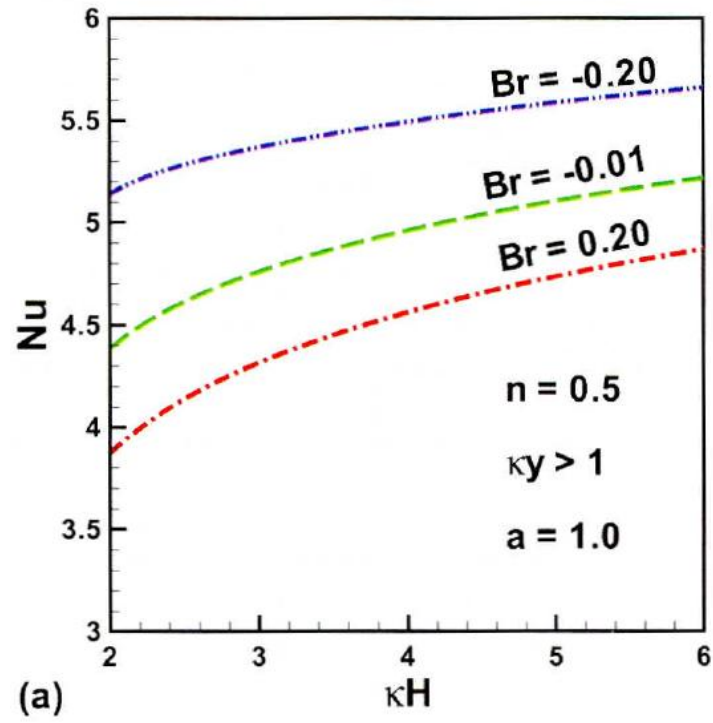


Figure 8. Effects of power-law index n and Br on dimensionless heat transfer rate when $\kappa y > 1$.